

CHEMISTRY

A European Journal



Accepted Article

Title: A Manganese(V)-Oxo TAML Cation Radical Complex: Synthesis, Characterization, and Reactivity Studies

Authors: Deepika G. Karmalkar, Xiao-Xi Li, Mi Sook Seo, Muniyandi Sankaralingam, Takehiro Ohta, Ritimukta Sarangi, Seungwoo Hong, and Wonwoo Nam

This manuscript has been accepted after peer review and appears as an Accepted Article online prior to editing, proofing, and formal publication of the final Version of Record (VoR). This work is currently citable by using the Digital Object Identifier (DOI) given below. The VoR will be published online in Early View as soon as possible and may be different to this Accepted Article as a result of editing. Readers should obtain the VoR from the journal website shown below when it is published to ensure accuracy of information. The authors are responsible for the content of this Accepted Article.

To be cited as: *Chem. Eur. J.* 10.1002/chem.201804898

Link to VoR: <http://dx.doi.org/10.1002/chem.201804898>

Supported by
ACES

WILEY-VCH

A Manganese(V)-Oxo TAML Cation Radical Complex: Synthesis, Characterization, and Reactivity Studies**

Deepika G. Karmalkar, Xiao-Xi Li, Mi Sook Seo, Muniyandi Sankaralingam, Takehiro Ohta, Ritimukta Sarangi,* Seungwoo Hong,* and Wonwoo Nam*

Abstract: A mononuclear manganese(V)-oxo complex bearing tetraamido macrocyclic ligand (TAML), $[\text{Mn}^{\text{V}}(\text{O})(\text{TAML})]^-$ (**1**), is a sluggish oxidant in oxidation reactions. Herein, we report a mononuclear manganese(V)-oxo TAML cation radical complex, $[\text{Mn}^{\text{V}}(\text{O})(\text{TAML}^{\bullet+})]$ (**2**), which is synthesized by reacting $[\text{Mn}^{\text{III}}(\text{TAML})]^-$ with 3.0 equiv of $[\text{Ru}^{\text{III}}(\text{bpy})_3]^{3+}$ or upon addition of one-electron oxidant to **1** and then characterized thoroughly with various spectroscopic techniques along with DFT calculations. While **1** is a sluggish oxidant, **2** is a strong oxidant capable of activating C-H bonds of hydrocarbons (i.e., hydrogen atom transfer reaction) and transferring its oxygen atom to thioanisoles and olefins (i.e., oxygen atom transfer reaction).

High-valent iron-oxo species and their manganese-oxo analogues have been invoked as reactive intermediates in the catalytic oxidation of organic substrates by metalloenzymes and synthetic metal catalysts.^{1,2} One notable example is the iron(IV)-oxo porphyrin π -cation radical species, referred to as compound I (Cpd I), in Cytochromes P450 (CYP450).¹ There is another high-valent iron-oxo intermediate found in heme enzymes; that is one-electron reduced species of Cpd I, which is iron(IV)-oxo porphyrin species, referred to as compound II (Cpd II).¹ The structural and chemical properties of Cpd I and Cpd II have been investigated intensively in enzymatic and biomimetic reactions over the past several decades; it is well known that Cpd I, iron(IV)-oxo porphyrin π -cation radical, is much more reactive than Cpd II, iron(IV)-oxo porphyrin, in oxidation reactions.¹

[*] D. G. Karmalkar, Dr. X.-X. Li, Dr. M. S. Seo, Dr. M. Sankaralingam, Prof. Dr. W. Nam
Department of Chemistry and Nano Science, Ewha Womans University, Seoul 03760, Korea, E-mail: wwnam@ewha.ac.kr

Dr. T. Ohta
Picobiology Institute, Graduate School of Life Science, University of Hyogo, RSC-UH LP Center, Hyogo 679-5148, Japan

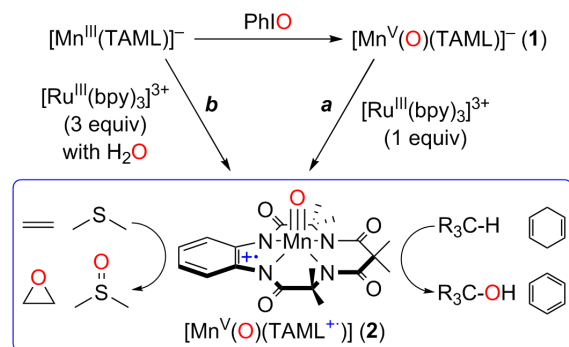
Prof. Dr. S. Hong
Department of Chemistry, Sookmyung Women's University, Seoul 04310, Korea, E-mail: hsw@sm.ac.kr

Prof. Dr. Ritimukta Sarangi
Stanford Synchrotron Radiation Lightsource, SLAC National Accelerator Laboratory, Stanford University, California 94025, USA
E-mail: ritis@slac.stanford.edu

[**] This work was supported by NRF of Korea through CRI (NRF-2012R1A3A2048842 to W.N.), GRL (NRF-2010-00353 to W.N.), MSIP (NRF-2017R1C1B2002037 to S.H.), and Sookmyung Women's University Grants (1-1603-2053 to S.H.). The SSRL SMB resource was supported by the NIH National Institute of General Medical Sciences (NIGMS) through a Biomedical Technology Research Resource P41 grant (P41GM103393) and by the DOE Office of Biological and Environmental Research.



Supporting information for this article is available on the WWW under <http://www.angewandte.org> or from the author.



Scheme 1. Synthesis and Reactivity of $[\text{Mn}^{\text{V}}(\text{O})(\text{TAML}^{\bullet+})]$ (**2**)

High-valent manganese(V)-oxo species have attracted much attention recently as plausible intermediates in the oxidation of organic substrates and the oxygen evolution reaction in Photosystem II (PSII).^{3,4} In biomimetic studies, a number of Mn(V)-oxo complexes have been synthesized and characterized structurally and/or spectroscopically.³ Interestingly, the synthetic Mn(V)-oxo complexes of porphyrin, corrole, corrolazine, and TAML ligands exhibited low reactivities in oxidation reactions.^{3c,5} In addition to the Mn(V)-oxo complexes, Mn(IV)-oxo ligand cation radical species, which are the valence tautomers of the Mn(V)-oxo intermediates, have been synthesized upon addition of Lewis or Brønsted acids to the Mn(V)-oxo complexes of corrole and corrolazine, and reactivities of the Mn(V)-oxo and Mn(IV)-oxo ligand cation radical complexes were compared in hydrogen atom transfer (HAT) and oxygen atom transfer (OAT) reactions.⁶ Goldberg and co-workers synthesized a novel Mn(V)-oxo corrolazine cation radical complex upon one-electron oxidation of its corresponding Mn(V)-oxo complex and discussed briefly their reactivities in OAT reaction.⁷

Very recently, we reported an iron(V)-imido TAML cation radical complex, $[\text{Fe}^{\text{V}}(\text{NTs})(\text{TAML}^{\bullet+})]$,^{8a} which was synthesized by oxidizing an iron(V)-imido complex, $[\text{Fe}^{\text{V}}(\text{NTs})(\text{TAML})]$,^{8b} with one-electron oxidants, such as $[\text{Fe}^{\text{III}}(\text{bpy})_3]^{3+}$, tris(4-bromophenyl)ammonium hexachloroantimonate $\{[(4\text{-BrC}_6\text{H}_4)_3\text{N}]\text{SbCl}_6\}$, and $[\text{Ru}^{\text{III}}(\text{bpy})_3]^{3+}$. In the study, we have demonstrated that the oxidation of $[\text{Fe}^{\text{V}}(\text{NTs})(\text{TAML})]$ occurs on the TAML ligand, not on the iron ion.^{8a} With this result and the report of Goldberg and co-workers,⁷ we attempted to oxidize the Mn(V)-oxo TAML complex, $[\text{Mn}^{\text{V}}(\text{O})(\text{TAML})]^-$ (**1**),^{5c} with one-electron oxidants. In this communication, we report the synthesis of a mononuclear manganese(V)-oxo TAML cation radical complex, $[\text{Mn}^{\text{V}}(\text{O})(\text{TAML}^{\bullet+})]$ (**2**), upon one-electron oxidation of **1** by $[\text{Ru}^{\text{III}}(\text{bpy})_3]^{3+}$ (Scheme 1, reaction pathway a). **2** was also generated by reacting $[\text{Mn}^{\text{III}}(\text{TAML})]^-$ with 3 equiv of $[\text{Ru}^{\text{III}}(\text{bpy})_3]^{3+}$ (Scheme 1, reaction pathway b). Then, **2** was characterized with various spectroscopic techniques, demonstrating that **2** is a manganese(V)-oxo TAML cation radical complex possessing a Mn-O triple bond with a short Mn-O bond distance (1.54 Å) and a Mn-O bond vibrational frequency at 996 cm^{-1} . Interestingly, while **1** is a sluggish

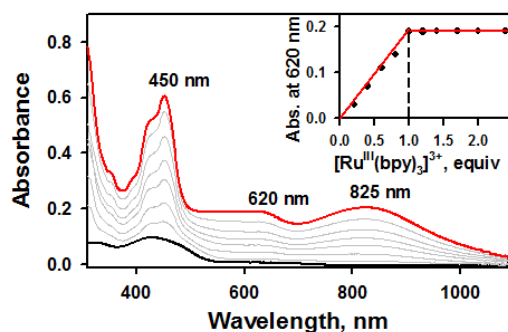


Figure 1. UV-vis spectral changes observed in the reaction of **1** (2.5×10^{-2} mM, black line) and $[\text{Ru}^{\text{III}}(\text{bpy})_3]^{3+}$ (3.0×10^{-2} mM) in CH_3CN at -40 °C. The peak at 450 nm was due to $[\text{Ru}^{\text{II}}(\text{bpy})_3]^{2+}$. Inset shows the plot of the absorbance change at 620 nm due to **2** upon addition of $[\text{Ru}(\text{bpy})_3]^{3+}$ to **1** (2.5×10^{-2} mM) in the increment of 0.2 equiv.

oxidant, **2** is a highly reactive oxidant that is capable of oxidizing hydrocarbon C-H bonds, thioanisoles, and olefins (Scheme 1, blue box). Some mechanistic aspects are also discussed in this study.

When $[\text{Mn}^{\text{III}}(\text{TAML})]^-$ was reacted with one-electron oxidant, such as $[\text{Ru}^{\text{III}}(\text{bpy})_3]^{3+}$ (>3 equiv), in the presence of H_2O in CH_3CN at -40 °C, we observed the formation of an intermediate with broad absorption bands at 620 and 825 nm (Supporting Information (SI), Figure S1). This intermediate was metastable at -40 °C but decayed fast at a higher temperature. Interestingly, this intermediate, denoted as **2**, was generated when $[\text{Mn}^{\text{V}}(\text{O})(\text{TAML})]^-$ (**1**) was treated with $[\text{Ru}^{\text{III}}(\text{bpy})_3]^{3+}$; addition of 1.2 equiv of $[\text{Ru}^{\text{III}}(\text{bpy})_3]^{3+}$ to a CH_3CN solution of **1** at -40 °C afforded the formation of **2** with electronic absorption bands at 620 nm ($\epsilon = 7600 \text{ M}^{-1} \text{ cm}^{-1}$) and 825 nm ($\epsilon = 8000 \text{ M}^{-1} \text{ cm}^{-1}$) (Figure 1, red line; also see SI, Experimental Section for the preparation of **1**). In contrast to $[\text{Ru}^{\text{III}}(\text{bpy})_3]^{3+}$ ($E_{\text{ox}} = 1.24 \text{ V vs SCE}$), other relatively weak one-electron oxidants, such as $[\text{Fe}^{\text{III}}(\text{bpy})_3]^{3+}$ ($E_{\text{ox}} = 1.06 \text{ V vs SCE}$) and tris(4-bromophenyl)ammonium hexachloroantimonate ($E_{\text{ox}} = 1.08 \text{ V vs SCE}$),⁹ did not convert **1** to **2** under the reaction conditions. These results can be interpreted with the electrochemical property of **1** that was determined with cyclic voltammetry; a quasi-reversible wave with the oxidation and reduction peak potentials at 1.21 V and 1.01 V (vs SCE), respectively, were determined in CH_3CN at -40 °C (SI, Figure S2). Since **2** was metastable ($t_{1/2}$ of ~40 min) at -40 °C, we were able to characterize it with various spectroscopic techniques.

X-band electron paramagnetic resonance (EPR) spectrum of a CH_3CN solution of **2** at 77 K exhibited a radical signal centered at $g = 2.002$ (SI, Figure S3a); EPR of **1** was silent.^{5e} The signal was quantified against an external standard, revealing a >80% yield of **2**. A cold spray ionization time-of-flight mass spectrum (CSI-MS) of **2** exhibited an ion peak at m/z of 546.4 in positive mode, whose mass and isotope distribution patterns correspond to $\{\text{Na}[\text{Mn}(\text{O})(\text{TAML})(\text{CH}_3\text{CN})_2]\}^+$ (calculated m/z of 546.1) (SI, Figure S3b). The ion peak of **2** shifted two-mass unit upon ^{18}O -substitution, confirming that **2** contains one oxygen atom in it (SI, Figure S3b, inset). Upon 441.6 nm-excitation, complex **2** exhibited an isotope-sensitive resonance Raman (rRaman) band at 986 cm^{-1} , which shifted to 945 cm^{-1} upon ^{18}O -substitution (SI, Figure S3c); these values are similar to those reported for **1** (e.g., 977 and 937 cm^{-1} for **1**- ^{16}O and **1**- ^{18}O , respectively).^{5e} The $\Delta_{160-180} = 41 \text{ cm}^{-1}$ is consistent with that calculated (44 cm^{-1}) from Hooke's law for a diatomic Mn-O oscillator.

Mn K-edge XAS and EXAFS measurements were performed on **1** and **2** to determine the geometric structure and oxidation state of **2**. The Mn K-edge XAS data in Figure 2a show no significant change

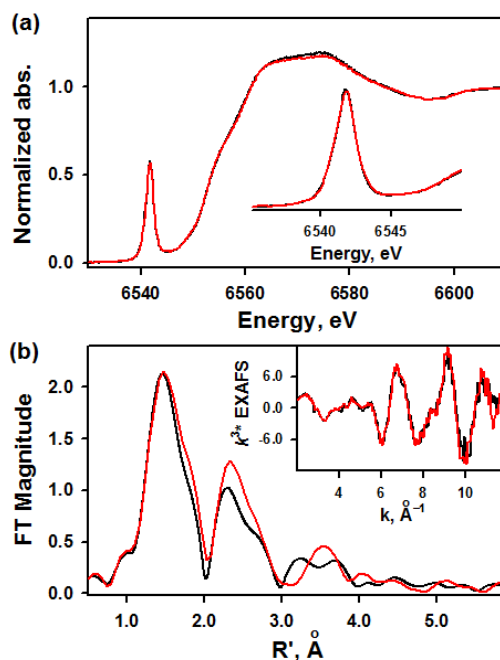


Figure 2. (a) The normalized Mn K-edge XAS data for **1** (black line) and **2** (red line). Inset shows the expanded pre-edge region. (b) Non-phase-shift corrected Fourier Transform data for **1** (black line) and **2** (red line). Inset shows the EXAFS comparison (SI, Figure S4).

at the Mn center upon oxidation with $[\text{Ru}^{\text{III}}(\text{bpy})_3]^{3+}$. This lack of spectral change at the pre-edge and rising-edge region indicates that the Mn center remains in the Mn(V) redox state and the oxidation occurs on the TAML ligand. This is also reflected in the comparison of the Mn K-edge EXAFS data for **1** and **2** and their respective Fourier transforms (Figure 2b and SI, Figure S4). The first shell is identical in both species, while small changes are observed in the outer shells dominated by TAML-based single and multiple scattering contributions. FEFF analysis of **1** and **2** confirmed very similar structures with 1 Mn-O at 1.54 \AA and 4 Mn-N at 1.88 \AA (SI, Table S1). While the second and third shell multiple scattering contributions are very similar in both fits, a larger contribution of outer-shell multiple-scattering is required to obtain a good fit for **2**, suggesting a change in the TAML ring upon oxidation.

To understand the electronic structure of **2**, density functional theory (DFT) calculations were performed at the UBP86/def2-TZVPP//def2-SVP level, and a doublet ground state was obtained (SI, Table S2). After analyzing the spin density distribution, we found that there was one spin located at the TAML ligand (SI, Table S3), which is in line with the experimental EPR result. In other words, **2** has an electronic configuration of $[\delta_{xy}^2, \pi_{xz}^0, \pi_{yz}^0, \sigma_{x^2-y^2}^0, \sigma_{z^2}^0, \pi_{\text{ligand}}^*]$, which has been confirmed by the orbital analysis results (SI, Figure S5). In calculations, the Mn-O bond vibrational frequency was found at 996 cm^{-1} , which shifted to 957 cm^{-1} upon ^{18}O substitution. This is in good agreement with the experimental rRaman data (e.g., the shift of 986 cm^{-1} to 945 cm^{-1} upon ^{18}O -substitution). In addition, similar to **1**,^{5e} the doublet ground state **2** with a Mn-O distance of 1.56 \AA (SI, Table S4) also has triple Mn-O bond character, which is also consistent with the EXAFS result (vide supra). Based on the results of the spectroscopic characterization and DFT calculations, we conclude that **2** is a Mn(V)-oxo TAML cation radical complex with a Mn-O triple bond.

We then investigated the reactivity of **2** in various oxidation reactions, such as C-H bond activation and the oxidation of thioanisole and olefin. While **1** was completely unreactive toward

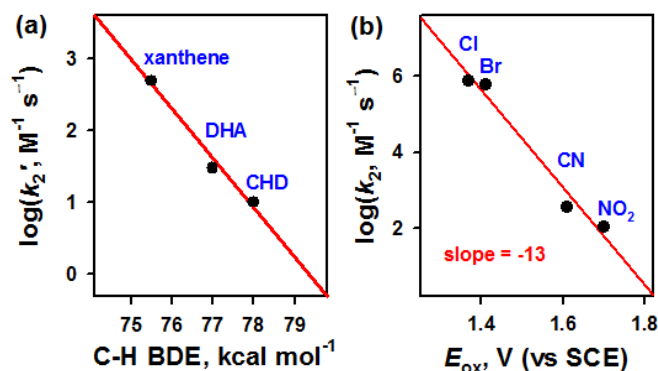


Figure 3. (a) Plot of $\log k_2'$ against C-H BDEs of substrates in the C-H bond activation reactions by **2** at -40°C (SI, Table S5). (b) Plot of $\log k_2$ against the E_{ox} values of *para*-X-substituted thioanisole (X = Cl, Br, CN, and NO₂) derivatives in the sulfoxidation reactions by **2** at -40°C (SI, Table S6).

substrates with weak C-H bonds, such as xanthene ($75.5 \text{ kcal mol}^{-1}$), 9,10-dihydroanthracene (DHA, 77 kcal mol^{-1}), 1,4-cyclohexadiene (CHD, 78 kcal mol^{-1}),¹⁰ even at room temperature, addition of CHD to a solution of **2** in CH₃CN at -40°C resulted in a rapid disappearance of absorption bands at 620 and 825 nm due to **2** (SI, Figure S6). Substrates having stronger C-H BDE such as fluorene (80 kcal mol^{-1}), triphenylmethane (81 kcal mol^{-1}) didn't react. The C-H bond activation reactions by **2** under pseudo-first-order conditions were monitored by UV-vis spectrophotometer. A linear dependence of the observed decay rate on CHD concentrations gave a second-order rate constant (k_2) of $4.0 \times 10 \text{ M}^{-1} \text{ s}^{-1}$ (SI, Table S5 and Figure S7). Product analysis of the xanthene oxidation by **2** revealed the quantitative formation of xanthone (48(2)% yield). When the xanthene oxidation was performed with $\sim 80\%$ ¹⁸O-labeled **2** (i.e., **2**-¹⁸O), $>75\%$ ¹⁸O was found in the xanthone product (SI, Figure S8). This result indicates that the oxygen atom in the product derived from the Mn-oxo oxidant. We also found that [Mn^{III}(TAML)]⁻ was formed as the decay product of **2** (SI, Figure S9); it may be proposed that [Mn^{IV}(TAML)] was the product but decayed to [Mn^{III}(TAML)]⁻ fast due to its instability. A kinetic isotope effect (KIE) value of 4.1(5) was determined in the oxidation of xanthene and deuterated xanthene by **2** (SI, Figure S10). We also observed a linear correlation between the k_2 values and the C-H bond dissociation energies (BDEs) of substrates (Figure 3a; also see SI, Table S5 and Figure S7). Taken together, **2** is a competent oxidant in C-H bond activation reactions and a hydrogen atom (H-atom) abstraction from the C-H bonds of substrates by **2** is proposed as the rate-determining step.

While **1** was unreactive with thioanisole even at room temperature, **2** reacted extremely fast with thioanisole even at -40°C ; we could not follow the reaction even with a stopped-flow spectrophotometer. We therefore used less reactive *para*-X-substituted thioanisoles (X = Cl, Br, CN, and NO₂) as substrates (SI, Figure S11) and determined the second-order rate constants (k_2) for the sulfoxidation of *para*-X-thioanisoles by **2** at -40°C using a stopped-flow spectrophotometer (SI, Figure S12). When the k_2 values were plotted against one-electron oxidation potentials (E_{ox}) of *para*-X-substituted thioanisoles, a large negative slope of -13 was obtained (Figure 3b and SI, Table S6; also see SI, Figure S13), suggesting that the sulfoxidation of *para*-X-thioanisoles by **2** occurs via electron transfer, followed by oxygen atom transfer.¹¹ Furthermore, the product analysis of the reaction solution revealed the formation of PhS(O)CH₃ ($\sim 95(3)\%$ yield) and [Mn^{III}(TAML)]⁻ as organic and manganese products, respectively (SI, Figure S14);

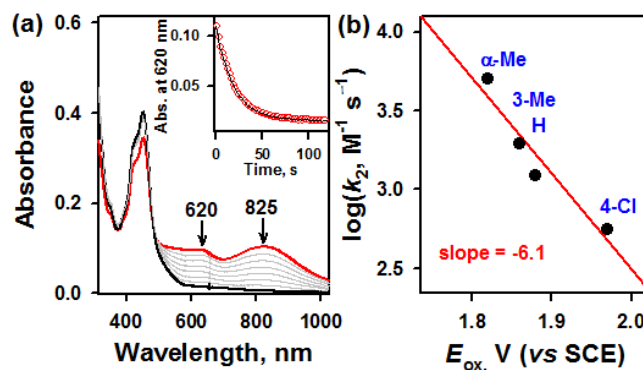


Figure 4. (a) UV-vis spectral changes observed in the reactions of **2** ($1.3 \times 10^{-2} \text{ mM}$) with 4-Cl-styrene ($6.3 \times 10^{-2} \text{ mM}$) in CH₃CN at -40°C . The peak at 450 nm was due to [Ru^{II}(bpy)₃]²⁺. Inset shows time trace monitored at 620 nm due to **2**. (b) Plot of $\log k_2$ against the E_{ox} values of X-substituted styrene (X = α -Me, 3-Me, H, and 4-Cl) derivatives in the epoxidation reactions by **2** at -40°C (SI, Table S7).

as discussed above, [Mn^{IV}(TAML)] may be the product which decays to [Mn^{III}(TAML)]⁻ fast due to its instability. When the sulfoxidation was performed with $\sim 80\%$ ¹⁸O-labeled **2**-¹⁸O, $>70\%$ ¹⁸O was found in the sulfoxide product (SI, Figure S15). The latter result suggests again that the source of the oxygen atom in the sulfoxide product was the Mn-oxo oxidant.

We finally investigated the olefin epoxidation using styrene and deuterated styrene as well as X-substituted (X = α -Me, 3-Me, H, and 4-Cl) styrenes. Upon addition of 4-Cl-styrene to the solution of **2** in CH₃CN at -40°C , **2** decayed with the first-order kinetics profile (Figure 4a), and the second-order rate constant of $1.2 \times 10^3 \text{ M}^{-1} \text{ s}^{-1}$ was determined in the reactions of styrene and styrene-*d*₈ at -40°C (SI, Table S7 and Figure S16). The KIE value of 1.0 suggests that the reaction of **2** with the styrene occurs via an OAT to the C=C double bond (SI, Figure S17). Product analysis by GC and GC-MS revealed that benzaldehyde (60(5)%) was formed as the major product with the formation of a small amount of styrene oxide (10(2)%). It has been well-documented that further oxidation of styrene oxide under acidic condition resulted in the formation of benzaldehyde.¹² When **2**-¹⁸O was used, the benzaldehyde product contained 70(5)% of ¹⁸O (SI, Figure S18), suggesting that the oxygen in the benzaldehyde product derived from **2**. A large negative slope of -6.1 was obtained by plotting $\log k_2$ values against one-electron oxidation potentials (E_{ox}) of X-substituted styrenes (Figure 4b), suggesting that **2** is capable of conducting olefin epoxidation reactions via electron transfer, followed by oxygen atom transfer.¹²

In summary, a mononuclear manganese(V)-oxo TAML cation radical complex, [Mn^V(O)(TAML^{•+})] (**2**), was successfully synthesized by oxidizing a manganese(V)-oxo complex, [Mn^V(O)(TAML)]⁻ (**1**), with one-electron oxidant. As shown in Cpd I and Cpd II in heme systems, **2** is much more reactive than **1** in HAT and OAT reactions. In future studies, we will focus on elucidating detailed reaction mechanisms of **2** in various oxidation reactions to compare with the chemistry of Cpd I in heme enzymes and models. Finally, we will pursue to synthesize a Mn(VI)-oxo complex, which is a valence tautomer of the Mn(V)-oxo TAML cation radical complex, by varying reaction conditions.

Received: ((will be filled in by the editorial staff))
Published online on ((will be filled in by the editorial staff))

Keywords: Manganese-Oxo Cation Radical • Cpd I vs Cpd II • C-H Bond Activation • Sulfoxidation • Olefin Epoxidation

- [1] a) P. R. Ortiz de Montellano, *Chem. Rev.* **2010**, *110*, 932; b) J. Rittle, M. T. Green, *Science* **2010**, *330*, 933; c) T. H. Yosca, J. Rittle, C. M. Krest, E. L. Onderko, A. Silakov, J. C. Calixto, R. K. Behan, M. T. Green, *Science* **2013**, *342*, 825; d) T. L. Poulos, *Chem. Rev.* **2014**, *114*, 3919; e) T. H. Yosca, A. P. Ledray, J. Ngo, M. T. Green, *J. Biol. Inorg. Chem.* **2017**, *22*, 209; f) X. Huang, J. T. Groves, *Chem. Rev.* **2018**, *118*, 2491.
- [2] a) W. Nam, Y.-M. Lee, S. Fukuzumi, *Acc. Chem. Res.* **2014**, *47*, 1146; b) S. A. Cook, A. S. Borovik, *Acc. Chem. Res.* **2015**, *48*, 2407; c) M. Puri, L. Que, Jr., *Acc. Chem. Res.* **2015**, *48*, 2443; d) K. Ray, F. Heims, M. Schwalbe, W. Nam, *Curr. Opin. Chem. Biol.* **2015**, *25*, 159; e) W. Nam, Y.-M. Lee, S. Fukuzumi, *Acc. Chem. Res.* **2018**, *51*, 2014.
- [3] a) H.-Y. Liu, M. H. R. Mahmood, S.-X. Qiu, C. K. Chang, *Coord. Chem. Rev.* **2013**, *257*, 1306; b) T. Taguchi, K. L. Stone, R. Gupta, B. Kaiser-Lassalle, J. Yano, M. P. Hendrich, A. S. Borovik, *Chem. Sci.* **2014**, *5*, 3064; c) H. M. Neu, R. A. Baglia, D. P. Goldberg, *Acc. Chem. Res.* **2015**, *48*, 2754; d) W. Liu, J. T. Groves, *Acc. Chem. Res.* **2015**, *48*, 1727; e) R. A. Baglia, J. P. T. Zaragoza, D. P. Goldberg, *Chem. Rev.* **2017**, *117*, 13320.
- [4] a) T. J. Meyer, M. H. V. Huynh, H. H. Thorp, *Angew. Chem. Int. Ed.* **2007**, *46*, 5284; b) S. Romain, L. Vigara, A. Llobet, *Acc. Chem. Res.* **2009**, *42*, 1944; c) Y. Umena, K. Kawakami, J.-R. Shen, N. Kamiya, *Nature* **2011**, *473*, 55; d) N. Cox, D. A. Pantazis, F. Neese, W. Lubitz, *Acc. Chem. Res.* **2013**, *46*, 1588; e) N. Cox, M. Retegan, F. Neese, D. A. Pantazis, A. Boussac, W. Lubitz, *Science* **2014**, *345*, 804; f) M. Suga, F. Akita, K. Hirata, G. Ueno, H. Murakami, Y. Nakajima, T. Shimizu, K. Yamashita, M. Yamamoto, H. Ago, J.-R. Shen, *Nature* **2015**, *517*, 99; g) R. Gupta, T. Taguchi, B. Lassalle-Kaiser, E. L. Bominaar, J. Yano, M. P. Hendrich, A. S. Borovik, *Proc. Natl. Acad. Sci. USA* **2015**, *112*, 5319; h) J. D. Blakemore, R. H. Crabtree, G. W. Brudvig, *Chem. Rev.* **2015**, *115*, 12974; i) D. J. Vinyard, G. W. Brudvig, *Annu. Rev. Phys. Chem.* **2017**, *68*, 101.
- [5] a) Z. Gross, G. Golubkov, L. Simkhovich, *Angew. Chem. Int. Ed.* **2000**, *39*, 4045; b) D.-L. Popescu, A. Chanda, M. Stadler, F. T. de Oliveira, A. D. Ryabov, E. Münck, E. L. Bominaar, T. J. Collins, *Coord. Chem. Rev.* **2008**, *252*, 2050; c) H. M. Neu, T. Yang, R. A. Baglia, T. H. Yosca, M. T. Green, M. G. Quesne, S. P. de Visser, D. P. Goldberg, *J. Am. Chem. Soc.* **2014**, *136*, 13845; d) R. A. Baglia, K. A. Prokop-Prigge, H. M. Neu, M. A. Siegler, D. P. Goldberg, *J. Am. Chem. Soc.* **2015**, *137*, 10874; e) S. Hong, Y.-M. Lee, M. Sankaralingam, A. K. Vardhaman, Y. J. Park, K.-B. Cho, T. Ogura, R. Sarangi, S. Fukuzumi, W. Nam, *J. Am. Chem. Soc.* **2016**, *138*, 8523.
- [6] a) C. J. Bougher, S. Liu, S. D. Hicks, M. M. Abu-Omar, *J. Am. Chem. Soc.* **2015**, *137*, 14481; b) J. P. T. Zaragoza, R. A. Baglia, M. A. Siegler, D. P. Goldberg, *J. Am. Chem. Soc.* **2015**, *137*, 6531; c) R. A. Baglia, C. M. Krest, T. Yang, P. Leeladee, D. P. Goldberg, *Inorg. Chem.* **2016**, *55*, 10800.
- [7] K. A. Prokop, H. M. Neu, S. P. de Visser, D. P. Goldberg, *J. Am. Chem. Soc.* **2011**, *133*, 15874.
- [8] a) S. Hong, X. Lu, Y.-M. Lee, M. S. Seo, T. Ohta, T. Ogura, M. Clémancey, P. Maldivi, J.-M. Latour, R. Sarangi, W. Nam, *J. Am. Chem. Soc.* **2017**, *139*, 14372; b) S. Hong, K. D. Sutherlin, A. K. Vardhaman, J. J. Yan, S. Park, Y.-M. Lee, S. Jang, X. Lu, T. Ohta, T. Ogura, E. I. Solomon, W. Nam, *J. Am. Chem. Soc.* **2017**, *139*, 8800.
- [9] N. G. Connelly, W. E. Geiger, *Chem. Rev.* **1996**, *96*, 877.
- [10] Y.-R. Luo, In *Handbook of bond dissociation energies in organic compounds*, CRC Press, Boca Raton, **2003**, p. 380.
- [11] Y. Goto, T. Matsui, S.-i. Ozaki, Y. Watanabe, S. Fukuzumi, *J. Am. Chem. Soc.* **1999**, *121*, 9497.
- [12] J. Park, Y.-M. Lee, K. Ohkubo, W. Nam, S. Fukuzumi, *Inorg. Chem.* **2015**, *54*, 5806.

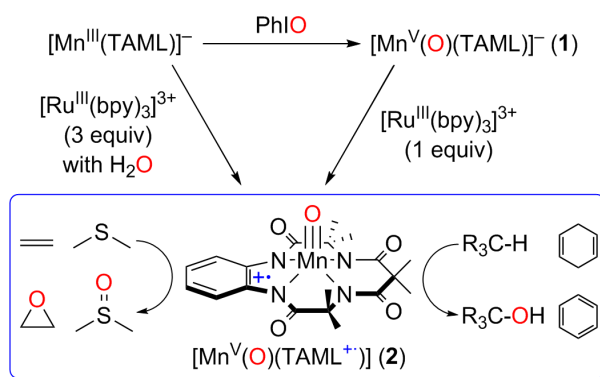
Entry for the Table of Contents

Manganese-Oxo

Deepika G. Karmalkar, Xiao-Xi Li, Mi Sook Seo, Muniyandi Sankaralingam, Takehiro Ohta, Ritimukta Sarangi,* Seungwoo Hong,* and Wonwoo Nam*

Page – Page

A Manganese(V)-Oxo TAML Cation Radical Complex: Synthesis, Characterization, and Reactivity Studies**



A mononuclear manganese(V)-oxo TAML cation radical complex, $[\text{Mn}^{\text{V}}(\text{O})(\text{TAML}^+)]$, is synthesized and characterized with various spectroscopic techniques along with DFT calculations. This Mn-oxo intermediate is a strong oxidant capable of activating C-H bonds of hydrocarbons (i.e., hydrogen atom transfer reaction) and transferring its oxygen atom to thioanisoles and olefins (i.e., oxygen atom transfer reaction).